A Multi-Cell RF Photoinjector Design*

Sanghyun Park
Department of Physics, University of California
Los Angeles, California 90024±1547

Abstract

A research and development effort has been underway to realize a high-brightness, low-emittance rf photoinjector to produce 1 to 3 nC bunch of photoelectrons at an energy of up to 20 MeV with a normalized rms emittance of 10 π mm±mrad or less. It consists of a half cell at the photocathode and seven full cells, operating in 2856 MHz, π±mode, standing wave. Numerical calculations with POISSON/SUPERFISH and PARMELA codes indicate that the design goal can be achieved within realistic constraints on mechanical device tolerances and rf source availability. The latest among the series of numerical models is somewhat similar to the SLAC type accelerator in geometric dimensions, although the device characteristics are vastly different.

I. INTRODUCTION

In order to raise the gain of a free-electron-laser oscillator/ampli®er, or to increase the luminosity in high-energy particle colliders, it is compelling to produce a low-emittance, high-brightness electron beam. Since the emittance is approximately an invariant in a drift space, it must be kept low during acceleration, especially when the electrons are non-relativistic. The BNL type $1\frac{1}{2}$±cell gun has a dipole mode caused by the side coupling of rf to the cells which gives rise to emittance growth. The BNL/SLAC/UCLA rf gun [1] is believed to improve the situation by eliminating the asymmetry at the ®rst cell and through higher gradient at the cathode. The energy at the exit, however, is still too low to drive even an infrared FEL so that one needs to append a linac, standing or travelling wave, to boost the energy at the cost of structural complexity and added expense. The AFEL [2] of LANL is a compact system without an additional booster linac, and it is a complicated structure. Even fabricating a copy of it will be quite involved. Therefore it is desirable to design a simple system that meets the performance requirements. The design reported here contends to be such a device.

II. BOUNDARY CONDITIONS

Unlike an accelerator with open boundaries both at the entrance and the exit, an injector has a longitudinally asymmetric boundary condition. The ®eld balance among the cells can be achieved by adding a half cell at the end [3]. This turns out to be quite arti®cial; when an opening of adequate size is made for particle exit, the broken symmetry forces the rf power to accumulate near the cathode [4] and it decays out as one moves away from it. Similar ®eld unbalance can be seen at the photoinjector of the APEX [5] system. The recipe to avoid this problem is as follows. A number of full cells are connected in series and a half cell is added at either end, as mentioned above. Adjust the inner radius of all cells by the same amount for a correct resonance frequency and mode separation. Take one full cell out. This has an individual resonance frequency f_r, different from that of the assembly. Prepare a full cell with an identical aperture to others on one side, but with a long drift, which serves as an rf choke as well as a beam exit, on the other. Tune the frequency of this cell to f_r using the inner diameter as a control knob. Then add to the rest of the assembly. A ®ne tuning of the last cell must be done to maintain the overall resonance frequency and ®eld balance.

Overall length	42.0 cm
Full cell length	5.250 cm
Cell diameter	8.2220 cm
Last cell diameter	8.2006 cm
Iris diameter	2.400 cm
Iris radius of curvature	0.3200 cm
Disk thickness	0.6400 cm

Table I
Geometric dimensions of the $7\frac{1}{2}$±cell injector

III. SUPERFISH RESULTS

The geometric parameters obtained through the procedures described above are shown in Table I, and the distribution of the accelerating ®eld along the axis is shown in Fig 1. With the dimensions shown above as input, the SUPERFISH code [6] produced the ®eld distribution inside the cavity that can be approximately represented by

$$E_z(z) = E_0 \sin(kz)$$

where the axial ®eldE_0=97 MV/m at $r = 0$ for the input power of 24 MW, $k = 2\pi f_0/c$ is the wavenumber for the frequency f_0=2.856 GHz. The electrical characteristics of the design is summarized in Table II.

IV. CONSIDERATIONS AT HIGH POWER

The disk thickness is comparable to those in the SLAC travelling wave structure, and much thinner than either BNL [7] or Grumman/BNL gun [8] disks. The latter, a 3±1/2 cell injector, has water channels to remove the dissipated heat from the disks at high duty cycle. The present design has the surface power dissipation of about 3 kW/cm^2 around the iris, and twice as much at the rest of the disk. This rate goes up to 15 kW/cm^2 at the wall with the input power of 24 MW. With a duty cycle low enough, say 10 pulses per second, cooling and tuning by temperature control will be less of a problem. If the maximum surface ®eld is too high at the operating rf power level, it may be the source of dark

*Work supported by the U. S. Department of Energy, under Grant DE±FG03±92ER±40493

Resonance freq.	2856 MHz
Separation to next mode	1.3 MHz
Cavity Q, unloaded	17,200
Transit time factor	0.737
Effective shunt impedance	45.3 MΩ/m
Input rf power	24 MW
Accel. ®eld at cathode	97 MV/m
Max. surface ®eld	134 MV/m

Table II
Summary of SUPERFISH results for the device, with the driving input rf power of 24 MW

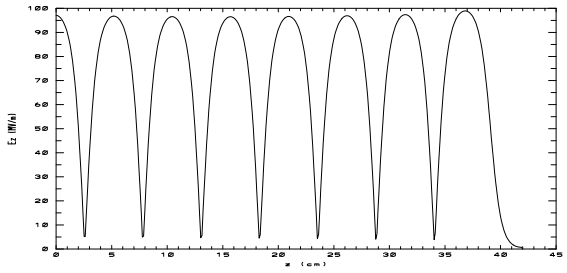

Figure 1. Magnitude of the accelerating ®eld in MV/m for z=0 to 45cm. The full scale is 100MV/m, and the last cell ends at 39cm.

current, or it may cause a breakdown. From the SUPERFISH result, it is about 130 MV/m, not too high to be a cause for concern. Another factor of practical importance is the available length of the high-power rf pulse. The ®ll time is, in the case of a standing-wave structure, $\tau_{fill} = Q_L/\omega$ where Q_L is the loaded Q. If the rf power is critically coupled, Q_L is one half times the unloaded Q, leading to a ®ll time of about 0.5μs at $\omega/2\pi$=2.856 GHz.

V. PARTICLE DYNAMICS

With a photoelectron bunch of a few nanoCoulombs over the bunch length of a few picoseconds, the space-charge forces become dominant in the emittance growth. For a photoinjector, a compensation is done by applying a solenoidal focusing ®eld over the ®rst few cells. In this case the axial ®eld is nulled out at the cathode by a bucking coil. Although this method was shown to be effective, it is not a part of the injector. It can be added on for the optimization of the beam characteristics. The phase of the rf when the photoelectrons are emitted is an important parameter. Again, it can be experimentally chosen for either highest particle energy or the lowest energy spread. Without regard to these points, the PARMELA code was used for the purpose of demonstration. For an electron bunch of 3 nC, 2 mm radius, and 3.5 ps length, 2000 particles were followed throughout the 40 cm long injector followed by the drift space of 60 centimeters. At about z =55 cm, the particle losses begin to occur and continues to the end, where about 80% of the charge is left. The initiation of the particle loss is accompanied by a slight increase in the transverse rms beam size and a sharp decrease in normalized emittance in x and y. At the injector exit, the emittance is about 35 mm±mrad. It increases a few percent over a 10 cm distance. For almost linear increase in beam size by a small fraction and about same rate of particle loss, the emittance is lowered by more than factor of ®ve. This seems to indicate that the largest contribution in emittance is from those uncorrelated in phase space. Nevertheless, the rest of the bunch propagates along the drift space with most of the charge still retained. The energy spread is on the order of a few percent in the acceleration period. At the exit, it is about 0.3%, and at the end of the simulation, it is lowered to 0.12%. The ®nal momentum of the beam was 23.5 MeV/c. During the drift the bunch length was shortened to the ®nal value of 2 ps whereas it was a steady 3.6 ps during the acceleration phase. The plots of these parameters are shown in Figs 2 through 7.

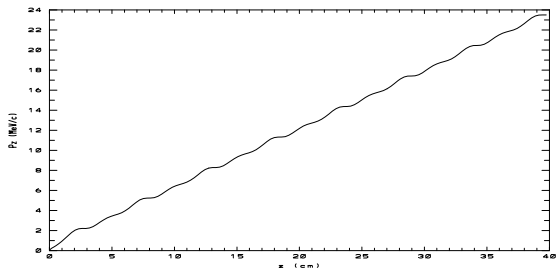

Figure 2. Electron momentum in MeV/c. At z= 40cm, P_z=23.5MeV/c

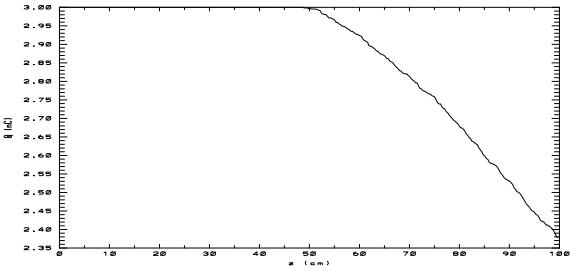

Figure 3. Charge in nC of the photoelectron bunch for z=0 to 100 cm. At z=100 cm, about 80% of the original charge of 3nC is retained.

VI. COUPLING AND OTHER ASPECTS

In principle, the rf power may be introduced into the cavity in many ways. The BNL gun employs magnetic coupling to suppress a zero-mode by driving both cells, whereas the new design calls for the full-cell drive to minimize the dipole-mode effect. The same rationale may be applied for the 7±1/2 cell structure,

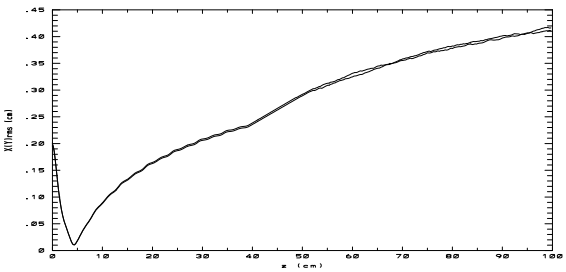

Figure 4. Transverse sizes of the bunch x_{rms} and y_{rms} in cm. At z=1m, they are bout 0.4 cm.

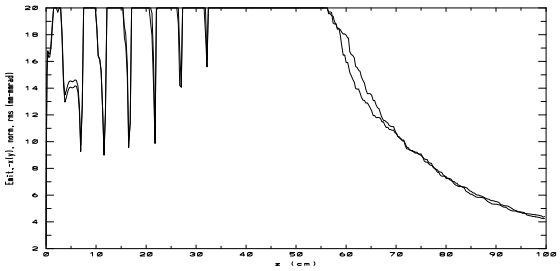

Figure 5. The normalized rms emittances in x and y. At z=1m, they are about 4 mm-mrad.

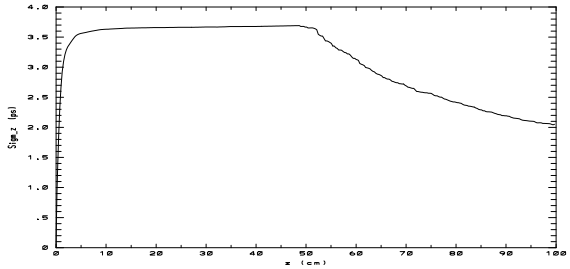

Figure 6. The bunch length in picoseconds. At z=1m, it is about 2 ps.

feeding the power through the last cell. In fact, a study was reported on driving a ®ve-cell superconducting cavity [9] from the downstream end of the structure. Whether electric coupling is better than magnetic coupling has to be resolved during the cold test.

VII. CONCLUSION

Based on the wave studies and particle simulations, an aluminum model has been made. Aside from the measurements of the ®eld structure through a bead pull method [10], there are a series of low-power tests possible. This series includes scattering parameter measurements in the steady state, and transient-coupling studies with pulsed low power at about 1 watt. Higher-order-mode outcoupling needs to be investigated if more than one microbunch is desired in every macropulse. While progress is still being made in the search for reliable photocathode materials with high quantum ef®ciency, it is equally important to explore an injector that is simple to manufacture, and which has high shunt impedance with lower content of unwanted modes.

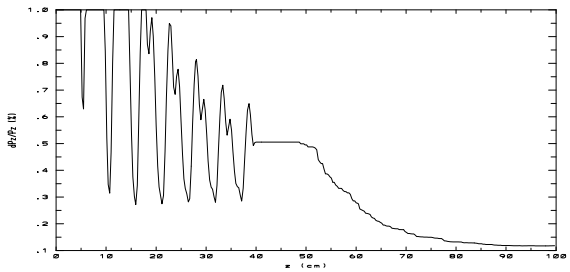

Figure 7. The energy spread in %. At z=1m, it is 0.12%.

References

[1] D. T. Palmer et al., These proceedings

[2] R. L. Shef®eld et al.,*NIM*, **A318**,182 (1992)

[3] S. Park and C. Pellegrini, Proc. 1993 Part. Accel. Conf., p. 570

[4] S. Park et al., Proc. 1994 Linac Conf., p. 280

[5] P. G. O'Shea et al., Proc. 1991 Part. Accel. Conf., p. 2754

[6] K. Halbach and R. F. Holsinger, *Particle Accelerators* **7**, 213 (1976)

[7] K. T. McDonald, IEEE Trans. Electron Dev. **ED-35**,2052 (1988)

[8] I. S. Lehrman et al., Proc. 1992 Linac Conf., p. 280

[9] Z. Li et al., Proc. 1993 Part. Accel. Conf., p. 179

[10] L. C. Maier and J. C. Slater, *Journal of Applied Physics*, Vol.**23**, Num**1** 69 - 77, Jan 1952